Hindawi
International Journal of Antennas and Propagation
Volume 2020, Article ID 8760297, 12 pages
https://doi.org/10.1155/2020/8760297

Research Article

Four-Element Microstrip Patch Array Antenna with Corporate-Series Feed Network for 5G Communication

Janam Maharjan and Dong-You Choi

Department of Information and Communications Engineering, Chosun University, Gwangju, Republic of Korea

Correspondence should be addressed to Dong-You Choi; dychoi@chosun.ac.kr

Received 23 January 2020; Accepted 13 April 2020; Published 27 April 2020

Academic Editor: Symeon Nikolaou

The paper proposes a simple four-element microstrip patch array antenna fed with corporate-series technique. The paper compares the proposed design with four-element antennas fed with only series-fed and corporate-fed microstrip antennas. All three antenna designs use rectangular microstrip patch elements with two insets and slots on both sides of the patch. The patch elements are accompanied by Yagi elements: three director elements and two reflector elements. Through comparison of simulation results, the paper shows that four-element array antenna with combined corporate-series feeding technique performs better compared to antennas with only either series or corporate feeding network. The proposed corporate-series fed antenna achieves better performance with wide frequency bandwidth of 25.04–30.87 GHz and gain of 9.5 dB. The antenna has an end-fire radiation pattern. Overall performance shows that the proposed corporate-series-fed microstrip patch antenna with Yagi elements is suitable for next generation 5G communication.

1. Introduction

Progress in the field of technology has become inevitable with the beginning of the industrial revolution. With the recent implementation of the 4th generation (4G) of mobile communication in many countries, the world is now shifting the focus to 5th generation (5G) for the future. Owing to the growth in mobile technology across the world and user demands for wireless devices and applications such as Internet of things (IoTs) that require higher bandwidths has led to a global bandwidth shortage for current wireless cellular networks. The 5G communication system is the answer to these new demands; this technology offers a larger spectrum and coverage, energy efficiency, and high data rate (10–50 Gbps), and the device density that it supports is higher than that supported by current 4G systems. The 5G system shall exploit millimeter-wave bands [1] and further improve the communication experience. The Third Generation Partnership Project (3GPP) has allocated the spectrum for 5G in two different frequency ranges. Frequency range 1 includes frequency bands below 6 GHz [2], and frequency range 2 includes frequency bands above 24 GHz and into the millimeter-wave range (24, 26, 28, and 39 GHz) [3].

Microstrip patch antennas have been preferred for antenna design because its characteristics are suitable for commercial wireless applications. They are smaller, lightweight, and easy to fabricate; they can have different shapes such as rectangular, square, and triangular, and they support high-density packaging. Patch antenna manufacturing cost is low. In [4], a wideband patch array is presented with modified unequal arms. In [5], 5G antenna with sector-disk radiating patch placed inside a circular-shaped slot is presented. Modification in the shape of patch antennas has helped to achieve desirable antenna performance. In addition, patch antennas support various feed techniques and can be developed into arrays to improve the gain and achieve the desired pattern requirements. Owing to these reasons, patch antennas have proven to be a strong candidate for millimeter-wave applications. Thus, 5G antennas have been developed using the microstrip patch technology. For better results, microstrip array antennas designed using various techniques have also been employed and researched for 5G applications [5–11].

Although millimeter waves are the future of wireless communication, they have few flaws. One of them is the significant free-space path loss caused by their high operating frequency [12]. Millimeter waves are also susceptible to high propagation loss because of atmospheric absorption. Thus, the factor of high propagation loss because of atmospheric absorption must be considered in the mm-waves antenna design [13]. However, the band of frequencies below 28 GHz is relatively less affected by atmospheric absorptions and has relatively less attenuations.

The easy feed technique is one of the useful characteristics of microstrip patch antennas in wireless applications. The microstrip patch elements of an array antenna can be fed using a single line or multiple lines depending on the requirement of the system. There are various complex types of feeding techniques as well. Reference [14] presented a four-element dual-band printed slot antenna array for 5G which is fed using a modified Wilkinson power divider. In [15], wideband E-shaped microstrip patch antenna with folded-patch feed in proposed. In both cases, the feeding techniques are of complex nature, whereasa series network is a simple type of feed network that consists of a continuous transmission line through which a proportion of energy is progressively coupled into each element of an array along the line. In [16], a series feed technique has been employed to feed a 4×4 planar microstrip array antenna with a modular structure and small dimension that can operate in 5G networks at 28 GHz. In [17], a modified 3×3 series-fed patch array antenna capable of beam steering is presented for 28 GHz millimeter-wave applications.

Corporate feed is a popular feed technique used for microstrip array antennas. In the case of corporate feed network, the power is equally split at each junction of the microstrip patch array antenna for uniform distribution. In [18], a 16-element patch array antenna suitable for 5G application is designed with a corporate feed network and is employed to achieve a bandwidth greater than 300 MHz. Some researchers have combined the series and corporate feed techniques to achieve the desired antenna outputs. In [19], a rectangular microstrip patch array antenna with a 16-element corporate-series feed network is proposed; it operates at 28 GHz for 5G applications. However, the antennas mentioned above individually achieved comparatively narrow bandwidths with series feed, corporate feed, or corporate-series feed networks.

Bearing in mind the above considerations, microstrip array antennas with three different feeding techniques are discussed in this study. Rectangular microstrip patch with multiple insets is used as the single patch element for the array antennas. Array antenna with only series feed and only corporate feed networks are designed and simulated, followed by the design of array antenna with combined corporate and series feed network. All three antennas are targeted to operate at a 28 GHz frequency band and produce end-fire radiation pattern for 5G communication. Yagi elements are also added to the designs to improve the overall gain and bandwidth. The detailed design of the array antenna shall be discussed in the subsequent sections of the paper.

2. Single Element Design

First, the single patch element to be implemented in arrays with different feeding techniques was designed. For the single patch rectangular element, tentative length and width of the patch were calculated as 1.64 and 3.23 mm, respectively, for an operating frequency of 28 GHz using a rectangular patch design equation [20]. However, to achieve the desired result of high bandwidth, the parameters of the single patch element were drastically optimized to 5.3 mm × 11 mm ($L_p \times W_p$). The thickness of the microstrip patch was 1.6 mm, and the overall parameter of the proposed antenna was 16 mm × 15 mm × 1.6 mm. The design was built on a substrate of Taconic RF-45 that has a dielectric constant (e_r) of 4.5 and loss tangent of 0.0037.

In the design, a simple inset of size 2.25 mm × 1.5 mm and an extra inset of size 3.5 mm × 0.25 mm were made on each side of the rectangular patch as seen in Figure 1. The addition of insets on the patch helped in achieving the operating frequency band of 28 GHz. Yagi elements were also added to the design to improve the bandwidth and overall gain. A pair of reflector elements were placed below the patch, and three director elements were placed above the patch. The distance between director elements and reflector elements was adjusted to achieve the desirable results. The geometry of the finalized single patch element with Yagi elements is shown in Figure 1, and the dimensions are listed in Table 1.

3. Array Antenna with Series Feed

3.1. Series-Fed Array Antenna Design. After designing a single patch element that achieved the targeted antenna performance, the patch elements were combined in the next step to form a four-element antenna. In the first experiment, the four patch elements were combined to form an array using a series feed network. The first patch was fed with a microstrip feedline of width 2.2 mm (W_f), which is the same as that of single element. The remaining three patches were subsequently fed through an optimized thin stub of width 0.2 mm (one-tenth of the size of the feedline, i.e., $W_f/10$). The parameters of each single patch elements were unchanged, whereas only the size of the overall antenna was changed. All the patch elements were arranged in series, separated by a distance of stub length (L_{st}). Different parameters for the length of the stub were tested to achieve wide bandwidth. Two reflector elements and three director elements of size similar to the ones in single patch element were placed below the patch element close to the microstrip feed and above the last patch element in the series, respectively. Thus, an array antenna with four single patches, Yagi elements, and a continuous ground plane capable of operating around the millimeter-wave spectrum was achieved.

When the patches are arranged in series, the width of the antenna is compromised. In the design, adding more patch elements in series to obtain a bigger array does not increase

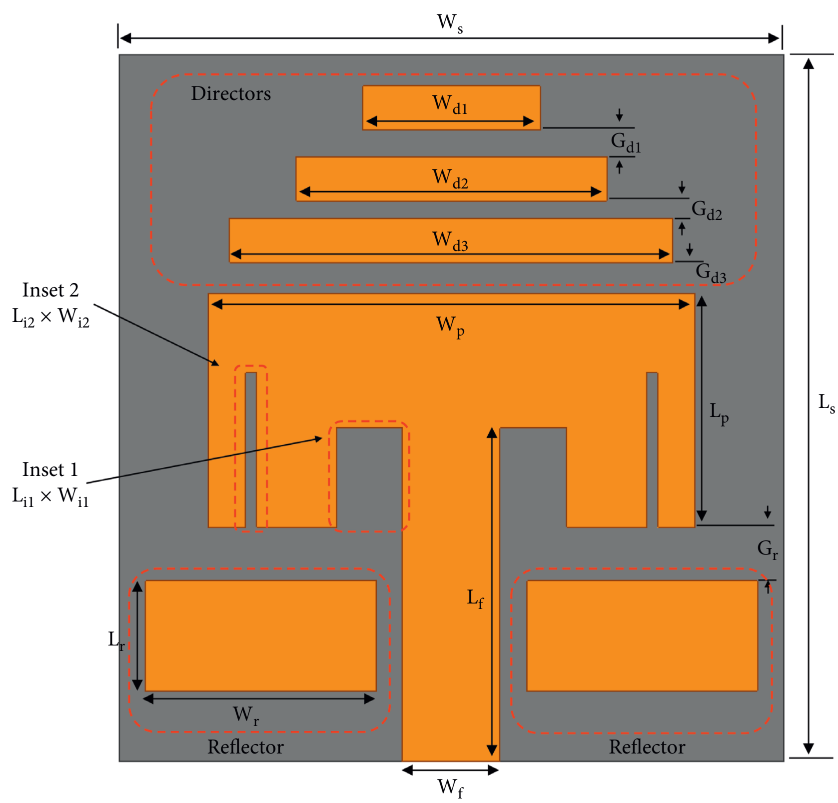

Figure 1: Geometry of single patch element with Yagi elements.

Table 1: Dimensions of the single patch element.

	Parameters	mm
Substrate	$L_s \times W_s$	16×15
Patch	$L_p \times W_p$	5.3×11
Ground	$L_g \times W_g$	16×15
Feedline	$L_f \times W_f$	7.55×2.2
Insets	$L_{i1} \times W_{i1}$	2.25×1.5
	$L_{i2} \times W_{i2}$	3.5×0.25
Reflector element	$L_r \times W_r$	2.5×5.2
	G_r	1.2
Director elements	W_{d1}, W_{d2}, W_{d3}	4, 7, 10
	L_d	1
	G_{d1}, G_{d2}, G_{d3}	0.6, 0.4, 0.7

the width of the antenna. However, the length of the antenna increases drastically, and the antenna performance is affected. The geometry of the array antenna with a series feed network is shown in Figure 2, and the additional dimensions are listed in Table 2.

3.2. Simulation Results and Discussions. A simple array antenna fed with the series feed technique with Yagi elements was designed and simulated in HFSS. The array antenna was simulated with different stub lengths. The stub length in which the bandwidth performance of the antenna was wide was chosen. As seen in Figure 3, S_{11} of the array antenna with stub lengths 2.2 mm, 3.2 mm, 4.2 mm, and 5.2 mm is shown. The return loss for the array antenna with stub length less than 3.2 mm produced comparatively narrower bands. Though the return loss is higher for stub lengths 4.2 mm and 5.2 mm, the bandwidth covered is narrower. Since, the target of the paper is to achieve wider bandwidth, stub length 3.2 mm was chosen for the antenna, which produced bandwidth of 25.6–30.3 GHz. Figure 4 shows the peak realized gain of the array antenna. The addition of Yagi elements not only increased the bandwidth but also improved the overall gain, with antenna achieving the highest peak realized gain of 7.98 dB at 29.3 GHz.

Typically, single patch elements are combined to obtain the final array antenna. Thus, in such cases, the return loss characteristics of an array antenna are similar to those of the single patch element. In the presented case, although most of the parameters of a single patch element are kept unchanged

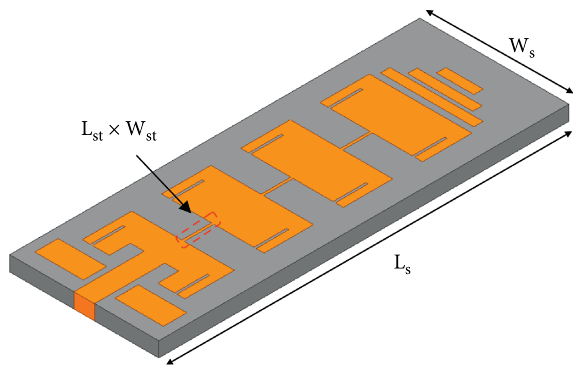

Figure 2: Geometry of series-fed microstrip array antenna.

Table 2: Dimensions of the series-fed microstrip array antenna.

	Parameters	mm
Substrate	$L_s \times W_s$	44×16
Stubs	L_{st} W_{st}	3.2 0.2 (W_f/10)

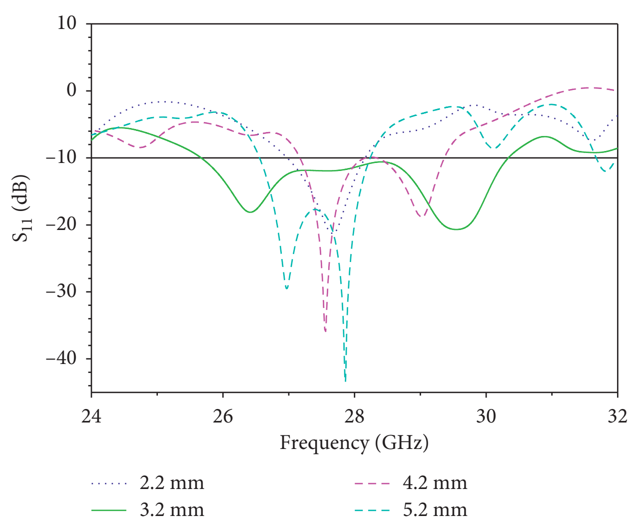

Figure 3: S_{11} of series-fed microstrip array antenna with stub lengths 2.2 mm, 3.2 mm, 4.2 mm, and 5.2 mm.

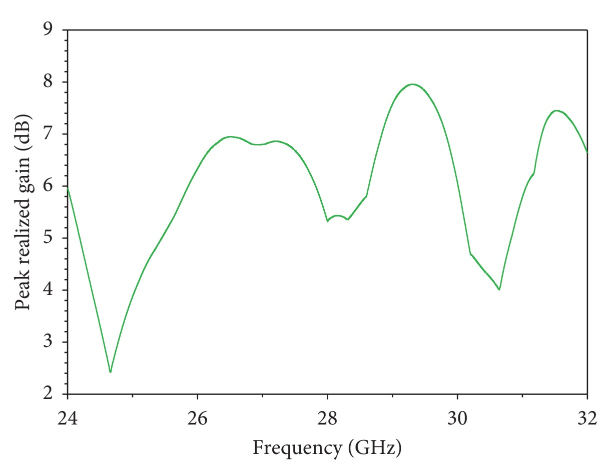

Figure 4: Peak realized gain of series-fed microstrip array antenna.

while designing the array antenna, the placement of Yagi elements in the array antenna is different. While the director elements of Yagi elements in a single patch are above the patch, director elements are placed only above patch element on the top of array antenna. Similarly, the reflector elements are placed only below first patch of the series array. Because of these changes, the return loss characteristics of the array antenna are different from that of a single patch element.

Figure 5 shows the radiation patterns of the array antenna at 26.4 GHz, 28 GHz, and 29.4 GHz. As seen from the plot, the antenna has achieved end-fire radiation pattern at higher frequencies with the employment of Yagi elements to the design. The radiation patterns closer to lower cut off frequencies were not desirable as seen at 26.4 GHz. The performance of the antenna is more directive at frequencies closer to upper cut-off frequencies. As seen at 28 GHz and 29.4 GHz, the antenna achieved end-fire radiation pattern.

4. Array Antenna with Corporate Feed

4.1. Corporate-Fed Array Design. For the second experiment, four patch elements were combined to obtain a corporate-fed array antenna. Similar to the series-fed array antenna, the parameters of the single patches and Yagi elements of the corporate-fed array antennas were kept same.

At first, the feedline was designed for which, by using microstrip formulas, the tentative width of the feedline was estimated around 3.03 mm [21] using the following equations:

$$\frac{w}{h} = \left[\frac{e^{H}}{8} - \frac{1}{4e^{H}}\right]^{-1},$$
$$H = \frac{Z_o\sqrt{2(\varepsilon_r + 1)}}{119.9} + \frac{1}{2}\left(\frac{\varepsilon_r - 1}{\varepsilon_r + 1}\right)\left(\ln\frac{\pi}{2} + \frac{1}{\varepsilon_r}\ln\frac{4}{\pi}\right). \tag{1}$$

Using [22], a tentative length of the microstrip was found as 5.18 mm. In the beginning, the power divider was designed and tested, using the calculated parameters. Later, the parameters were optimized to achieve desirable results. The width of the first feedline was changed from 3.03 mm to 2.2 mm, while the width of the second feedline was set to the value of λ_g, that is, 5 mm. Different lengths of the first feedline were simulated during the design, and the one that resulted in the desirable output was selected. The length of the second feedline is equal to one-fourth of the length of the first feedline (i.e., $L_{f2} = L_{f1}/4$). The T-junction opens into two sections. The total size of the feed of the primary T-junction is 2.2 mm × 30.6 mm, thereby making the distance between two secondary T-junction power dividers almost equal to $6\lambda_g$. The parameters of the feedlines of the secondary T-junction power divider are the same as that of the primary. Further, two single patch elements were placed on top of each secondary T-junction power divider, thereby making four single patch elements. Here, the distance between the two patch elements in a secondary T-junction power divider is 17.2 mm ($3\lambda_g$ + feedline width of single patch element). The triangular slits were also made in the center of the T-junction to improve the return loss characteristics of the antenna.

The parameters of the single patch element are the same for all. The dimensions of the director elements and reflector elements of the Yagi elements are also the same as that of the single patch element. The director elements are placed above every patch element, whereas the reflector elements are placed only at the open end of the single patch. Thus, each single patch is accompanied by only one reflector element below it. The geometry of the corporate-fed array antenna is shown in Figure 6, and the dimensions are listed in Table 3.

4.2. Simulation Results and Discussions. The corporate-fed array antenna with Yagi elements was designed and simulated in HFSS. Figure 7 shows the return loss of the antenna with different lengths of the first feedline, that is, L_{f1}. Three different lengths were chosen for the test. At first, antenna was simulated with the feedline length same as the length of the single patch element, that is, 5.3 mm. Then, the antenna was tested with the length of first feedline (L_{f1}) and one-fourth the width of first feedline more or less, that is, 5.85 mm ($L_{f1} + W_{f1}/4$), 4.75 mm ($L_{f1} - W_{f1}/4$). The length of the second feedline (L_{f2}) was set one-fourth of the length of the first feedline (i.e., $L_{f2} = L_{f1}/4$). As observed in the figure, the return loss of the array antenna produced multiple bandwidths when the lengths of the first feedline were 5.3 mm and 5.85 mm. Thus, the length for the first feedline, L_{f1}, is set as 4.75 mm, in which the return loss is less than -10 dB from 24.85 GHz to 30.32 GHz. Figure 8 shows the peak-realized gain, and as seen in the figure, the antenna achieved the highest peak realized gain of 8.8 dB at 26.7 GHz (inside the operating bandwidth). The addition of Yagi elements improved the gain of the overall operating region of the antenna.

Figure 9 shows the radiation pattern of array antenna at 26.7 GHz, 28 GHz, and 29.7 GHz. As seen from the plots, the array antenna's radiation pattern is similar to the ones with series-fed array antenna. However, the antenna shows directive characteristics at frequencies closer to lower cut-off region as well. In conclusion, the antenna achieved end-fire radiation pattern at higher frequencies, with slight improvement in overall radiation pattern compared to series-fed array antenna.

5. Array Antenna with Corporate-Series Feed

5.1. Design of Corporate-Series-Fed Array Antenna. After designing and testing series-fed and corporate-fed array antennas with Yagi elements, finally, the corporate and series feeding techniques were combined to form corporate-series-fed microstrip array antenna. Two patch elements are fed equal power of the 50-ohm source using a network of a microstrip line in the form of the T-junction power divider. Further, patch elements are added on top of each patch element in series using a quarter wavelength transformer stub.

The parameters of the patch elements are kept unchanged. The dimension of the Yagi elements are also kept

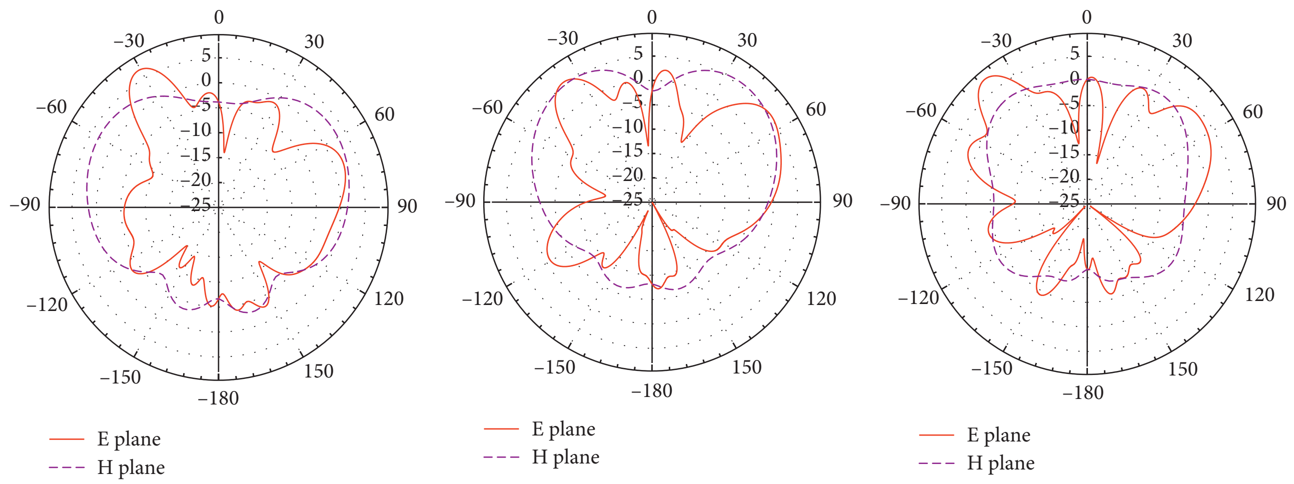

(a) (b) (c)

Figure 5: Radiation pattern of series-fed microstrip array antenna: (a) at 26.4 GHz, (b) at 28 GHz, and (c) at 29.4 GHz.

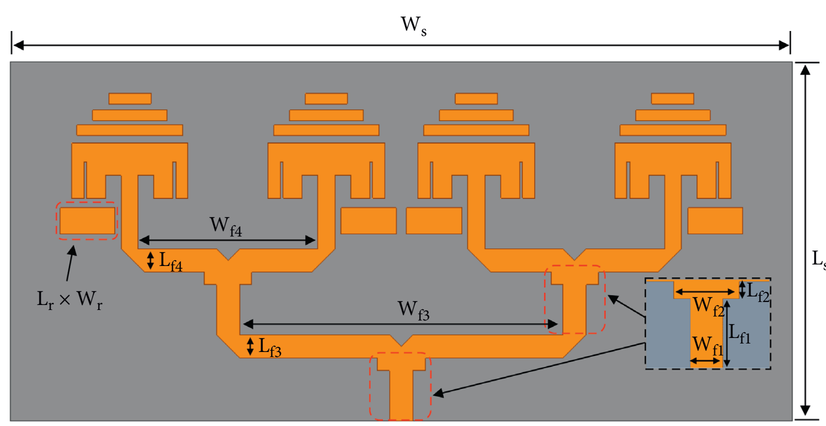

Figure 6: Geometry of corporate-fed microstrip array antenna.

Table 3: Dimensions of the corporate-fed microstrip array antenna.

	Parameters	Mm
Substrate	$L_s \times W_s$	36 × 74
Feedlines	$L_{f1} \times W_{f1}$ $L_{f2} \times W_{f2}$ $L_{f3} \times W_{f3}$ $L_{f4} \times W_{f4}$	4.75 × 2.2 1.18 × 5 ($L_{f1}/4 \times \lambda_g$) 2.2 × 30.6 2.2 × 17.2
Triangular slit (height × base)	$L_{f4} \times W_{f4}$	1.1 × 1.6
Reflector element	$L_r \times W_r$	2.5 × 5.2

the same as that in the single patch, series-fed antenna, and corporate-fed antenna. The width and length of the stub are the same as those in the series-fed array antenna. The dimension of the T-junction power divider is also the same as that of the T-junction of corporate-fed array antenna. The combination of series and corporate feeding techniques is done to enhance the overall performance of the antenna, decrease the size, increase the bandwidth, and improve the gain of the antenna, thereby making the array antenna suitable for 5G applications. In this way, two feeding techniques (i.e., series and corporate) are combined to obtain a corporate-series feeding technique. This combination of feeding techniques allowed us to design an array antenna of four patch elements without compromising on the overall size. The total size of the array antenna is also smaller than that of series- or corporate-fed array antennas.

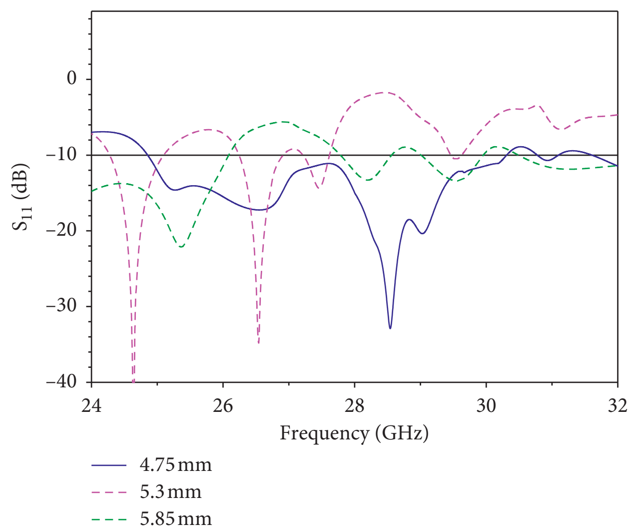

Figure 7: S_{11} of corporate-fed microstrip array antenna with feed lengths 4.75 mm, 5.3 mm, and 5.85 mm.

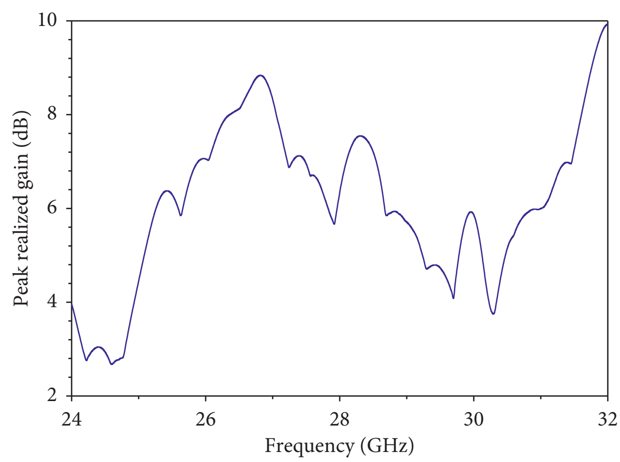

Figure 8: Peak realized gain of corporate-fed microstrip array antenna.

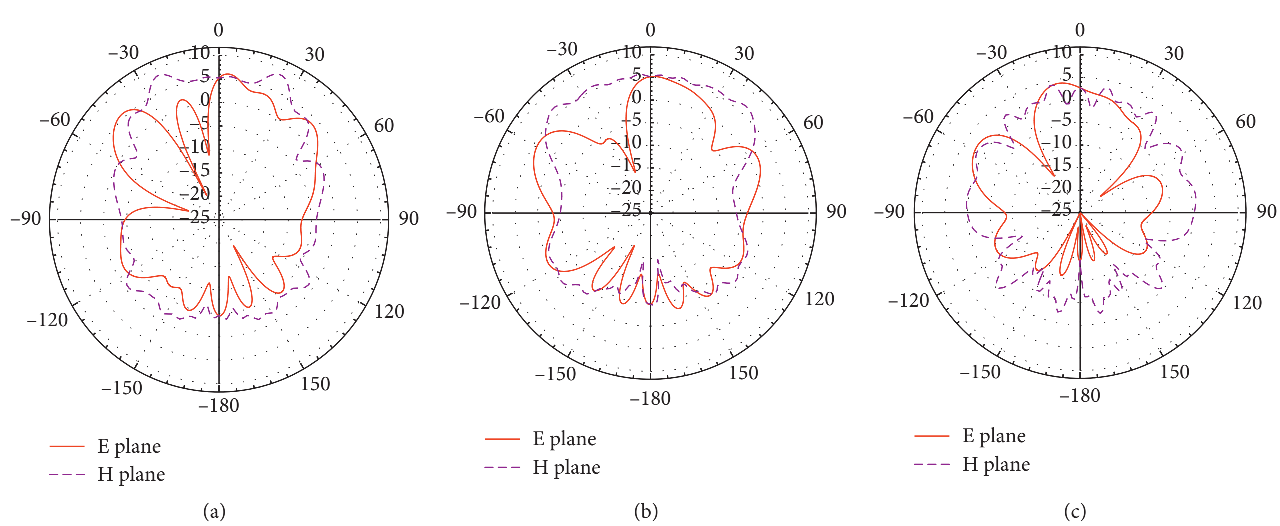

Figure 9: Radiation pattern of corporate-fed microstrip array antenna: (a) at 26.7 GHz, (b) at 28 GHz, and (c) at 29.7 GHz.

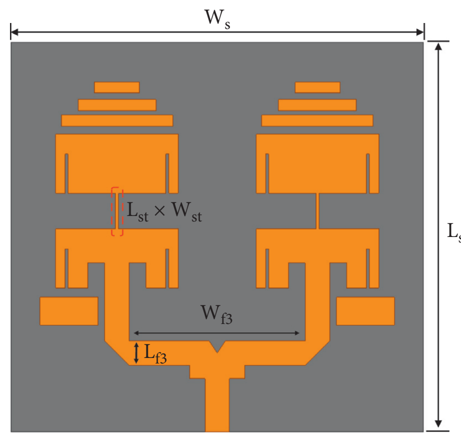

Figure 10: Geometry of proposed corporate-series-fed microstrip array antenna.

Table 4: Dimensions of the proposed corporate-series-fed array antenna.

	Parameters	mm
Substrate	$L_s \times W_s$	35×37
Feedlines	$L_{f3} \times W_{f3}$	2.2×15.8
Stubs	L_{st}	3.2
	W_{st}	0.2 ($W_f/10$)

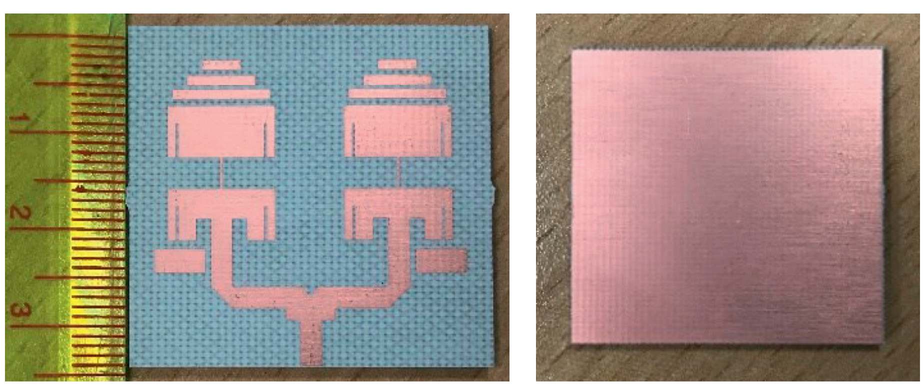

(a) (b)

Figure 11: Fabricated prototype of proposed corporate-series-fed microstrip array antenna: (a) top view and (b) bottom view.

The geometry of the proposed array antenna is shown in Figure 10, and the parameters are listed in Table 4. The fabricated prototype of the proposed corporate-series-fed microstrip array antenna is presented in Figure 11.

5.2. Results and Discussions. After simulating series- and corporate-fed array antennas, the proposed corporate-series-fed array antenna was finally designed and simulated; next, it was evaluated in a real environment. The measured and simulated S_{11} of the prototypes are presented in Figure 12 along with the simulated results of series- and corporate-fed array antennas. The measured return loss is below −10 dB from 25.8 GHz to 31.5 GHz. The array operates in a potential band proposed for 5G communication and even exhibits a return loss of approximately −27.7 dB at 27.7 GHz. However, in the simulated result, the return loss is around −48 dB at 27.8 GHz and is below −10 dB from 25.4 GHz to 30.87 GHz. This difference between the measured and simulated result could be due to minor manufacture defects, loss due to the nature of substrate, or loss due to connector. However, as can be observed in the figure, the return loss exhibits a matched behavior along the measured band.

In the proposed antenna, the fed power is first equally split at each junction of the patch array with uniform distribution; it passes along the continuous transmission lines

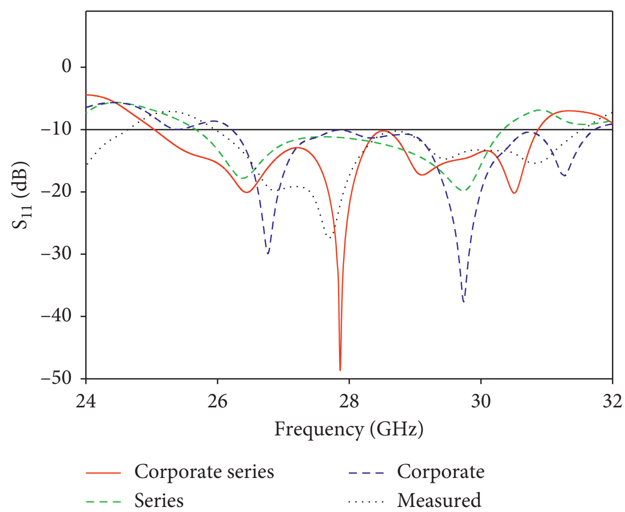

FIGURE 12: Measured and simulated S_{11} of proposed corporate-series-fed microstrip array antenna versus S_{11} of array antenna with series- and corporate- feed.

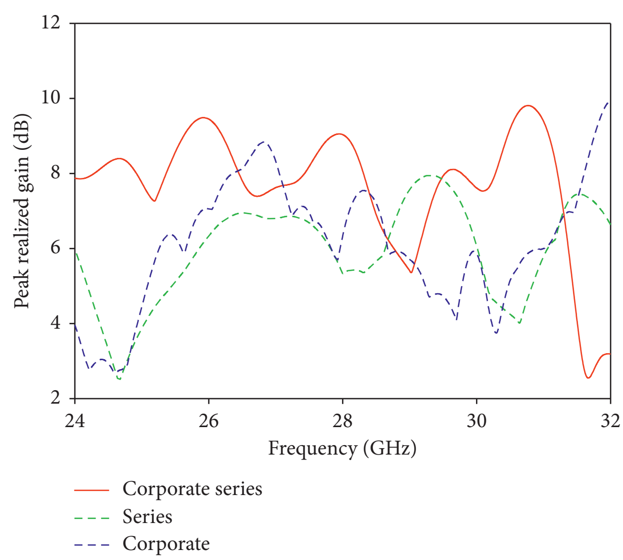

FIGURE 13: Peak realized gain of proposed microstrip array antenna with corporate-series, series-, and corporate feed.

through which a proportion of energy is progressively coupled into each element arranged in series. Owing to these reasons, an array antenna with high gain is achieved. Figure 13 depicts simulated results of peak-realized gain of the proposed array antenna along with results of series- and corporate-fed array antennas. We can observe that the realized gain of the proposed antenna over the operating frequency band of the antenna is higher than that of series- or corporate-fed array antennas.

Figure 14 shows the measured and simulated radiation patterns of the proposed corporate-series-fed array antenna at 27 GHz, 28 GHz, and 29 GHz. The measured radiation pattern is represented by broken lines while the simulated result is represented by a smooth straight line. As seen from the plot, the presented antennas exhibit a directional nature. Similar to series-fed and corporate-fed array antennas, the proposed array antenna shows end-fire radiation pattern, which is desired in mobile terminals, as it is immune from user shadowing [23]. Dissimilarities between the measured and simulated results are due to the loss because of manufacture defects, nature of substrate, or measurement errors.

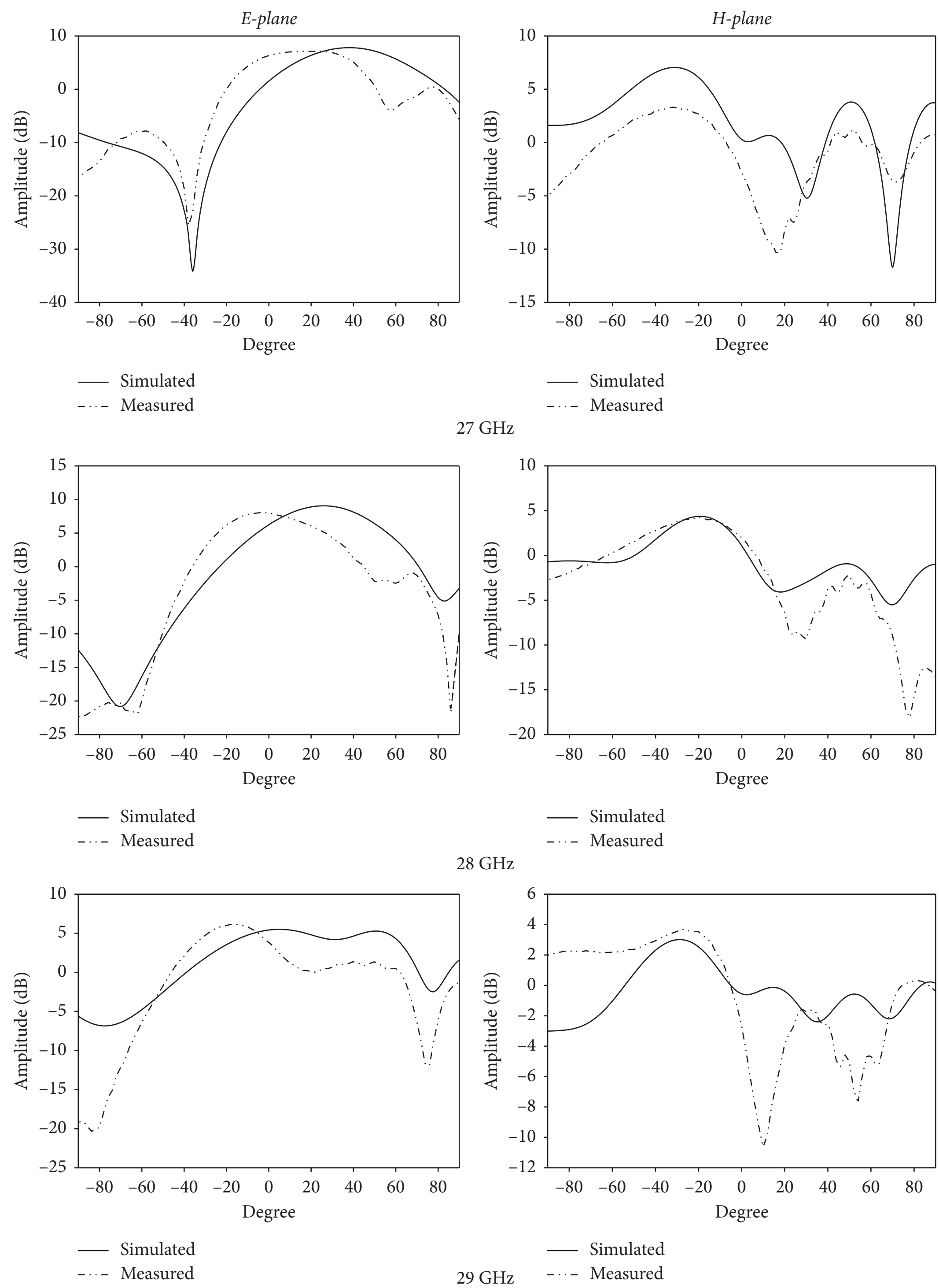

Figure 14: Radiation patterns of the proposed corporate-series-fed array antenna at 27 GHz, 28 GHz, and 29 GHz.

Table 5: Comparison between array antenna models.

Antenna type	Max. return loss (dB)	Bandwidth (GHz)	Max. gain (dB)	Size ($L_s \times W_s$) mm^2
Series feed	−20.7	25.67–30.34	7.98	44 × 16
Corporate feed	−32.9	24.85–30.32	8.85	36 × 74
Corporate-series feed	−48.6	25.05–30.87	9.49	35 × 37

Table 5 presents the comparison of array antennas with Yagi elements fed by series only, corporate only, and corporate-series feeding techniques in terms of maximum return loss, bandwidth, maximum peak realized gain, and size. From the comparison table, it is clear that the corporate-series-fed array antenna outperforms the series- and corporate-fed array antennas in terms of gain and bandwidth. In addition, the size of the antenna is smaller when the array is fed using the corporate-series feeding technique. This makes the proposed antenna suitable for smaller IOT devices equipped with 5G technology.

6. Conclusion

Designs of four-element patch antennas with series feed and corporate feed techniques are presented in this paper. Further, the feeding techniques were combined to form a corporate-series feed network, which was applied on the antenna design to propose a microstrip array antenna with wide bandwidth and end-fire radiation patterns. Further, Yagi elements were also added to the designs to improve the overall gain of the antenna. This paper presented the proposed design and further compared it with only series- and only corporate-fed array antennas. Overall, the simulation results proved that the proposed microstrip array antenna with corporate-series feed technique outperforms the series- and corporate-fed array antennas in terms of gain, size, and bandwidth. The proposed four-element antenna also covers most of the higher frequencies for 5G communication. The maximum peak realized gain of the antenna was 9.49 dB and achieved the wide bandwidth of 25.15–30.87 GHz.

Data Availability

The data used to support the findings of this study are included within the article.

Conflicts of Interest

The authors declare that they have no conflicts of interest.

Acknowledgments

This study was supported by the research fund from Chosun University, 2019.

References

[1] T. S. Rappaport, S. Sun, R. Mayzus et al., “Millimeter wave mobile communications for 5G cellular: it will work!” *IEEE Access*, vol. 1, pp. 335–349, 2013.

[2] 3GPP, “NR; User equipment (UE) radio transmission and reception; Part 1: range 1 standalone – rel. 15,” TS 38.101-1, 2019.

[3] 3GPP, “NR; User equipment (UE) radio transmission and reception; Part 2: range 2 standalone – rel. 15,” TS 38.101-102, 2019.

[4] S. Jam and H. Malekpoor, “Analysis on wideband patch arrays using unequal arms with equivalent circuit model in X-band,” *IEEE Antennas and Wireless Propagation Letters*, vol. 15, pp. 1861–1864, 2016.

[5] O. M. Haraz, M. M. M. Ali, S. Alshebeili, and A. Sebak, “Design of a 28/38 GHz dual-band printed slot antenna for the future 5G mobile communication Networks,” in *Proceedings of the 2015 IEEE International Symposium on Antennas and Propagation & USNC/URSI National Radio Science Meeting*, pp. 1532-1533, IEEE, Vancouver, BC, Cananda, October 2015.

[6] S. F. Jilani, Q. H. Abbasi, and A. Alomainy, “Inkjet-printed millimetre-wave PET-based flexible antenna for 5G wireless applications,” in *Proceedings of the 2018 IEEE MTT-S International Microwave Workshop Series on 5G Hardware and System Technologies (IMWS-5G)*, pp. 1–3, IEEE, Dublin, Ireland, October 2018.

[7] Y. Rahayu and M. I. Hidayat, “Design of 28/38 GHz dual-band triangular-shaped slot microstrip antenna array for 5G applications,” in *Proceedings of the 2018 2nd International Conference on Telematics and Future Generation Networks (TAFGEN)*, pp. 93–97, IEEE, Kuching, Malaysia, December 2018.

[8] H. A. Diawuo and Y.-B. Jung, “Broadband proximity-coupled microstrip planar antenna array for 5G cellular applications,” *IEEE Antennas and Wireless Propagation Letters*, vol. 17, no. 7, pp. 1286–1290, 2018.

[9] Q. Wang, N. Mu, L. Wang, S. Safavi-Naeini, and J. Liu, “5G MIMO conformal microstrip antenna design,” *Wireless Communications and Mobile Computing*, vol. 2017, Article ID 7616825, 11 pages, 2017.

[10] M. M. M. Ali and A. Sebak, “4×2-slot element for 30-GHz planar array antenna realized using SIW cavity and fed by microstrip line line-ridge gap waveguide,” in *Proceedings of the 2017 IEEE International Symposium on Antennas and Propagation & USNC/URSI National Radio Science Meeting*, pp. 2149-2150, San Diego, CA, USA, October 2017.

[11] M. M. M. Ali and A. Sebak, “Directive antennas for future 5G mobile wireless communications,” in *Proceedings of the 2017 XXXIInd General Assembly and Scientific Symposium of the International Union of Radio Science (URSI GASS)*, pp. 1–4, IEEE, Montreal, QC, Cananda, November 2017.

[12] J. Qiao, *Enabling Millimeter Wave Communication for 5G Cellular Networks: MAC-Layer Perspective*, University of Waterloo, Waterloo, Canada, 2015.

[13] E. E. Altshuler and R. A. Marr, “A comparison of experimental and theoretical values of atmospheric absorption at the longer millimeter wavelengths,” *IEEE Transactions on Antennas and Propagation*, vol. 36, no. 10, pp. 1471–1480, 1988.

[14] O. Haraz, M. M. M. Ali, A. Elboushi, and A. Sebak, “Four-element dual-band printed slot antenna array for the future 5G mobile communication networks,” in *Proceedings of the 2015 IEEE International Symposium on Antennas and Propagation & USNC/URSI National Radio Science Meeting*, pp. 1-2, Vancouver, BC, Canada, October 2015.

[15] H. Malekpoor and S. Jam, “Miniaturised asymmetric E-shaped microstrip patch antenna with folded-patch feed,” *IET Microwaves, Antennas & Propagation*, vol. 7, no. 2, pp. 85–91, 2013.

[16] T. Varum, A. Ramos, and J. N. Matos, “Planar microstrip series-fed array for 5G applications with beamforming capabilities,” in *Proceedings of the 2018 IEEE MTT-S International Microwave Workshop Series on 5G Hardware and System Technologies (IMWS-5G)*, pp. 1–3, IEEE, Dublin, Ireland, October 2018.

[17] M. Khalily, R. Tafazolli, T. A. Rahman, and M. R. Kamarudin, “Design of phased arrays of series-fed patch antennas with reduced number of the controllers for 28-GHz mm-wave applications,” *IEEE Antennas and Wireless Propagation Letters*, vol. 15, pp. 1305–1308, 2016.

[18] D. N. Arizaca-Cusicuna, J. L. Arizaca-Cusicuna, and M. Clemente-Arenas, "High gain 4x4 rectangular patch antenna array at 28GHz for future 5G applications," in *Proceedings of the 2018 IEEE XXV International Conference on Electronics, Electrical Engineering and Computing (INTERCON)*, pp. 1–4, IEEE, Lima, Peru, November 2018.

[19] B. T. Mohamed and H. Ammor, "A 16-elements corporate-series feed rectangular patch antenna array at 28GHz, for future 5G applications," in *Proceedings of the 2019 International Conference on Wireless Technologies, Embedded and Intelligent Systems (WITS)*, pp. 1–4, Fez, Morocco, April 2019.

[20] C. A. Balanis, *Antenna Theory: Analysis and Design*, pp. 811–876, John Wiley & Sons, Hoboken, NJ, USA, 2005.

[21] A. K. Rastogi, M. Bano, and S. Sharma, "Design and simulation model for compensated and optimized T-junctions in microstrip line," *International Journal of Advanced Research in Computer Engineering & Technology*, vol. 3, 2018.

[22] D. M. Pozar, *Microwave Engineering*, pp. 147–150, John Wiley & Sons, Hoboken, NJ, USA, 2009.

[23] I. Syrytsin, S. Zhang, and G. F. Pedersen, "Performance investigation of a mobile terminal phased array with user effects at 3.5 GHz for LTE advanced," *IEEE Antennas and Wireless Propagation Letters*, vol. 16, pp. 1847–1850, 2017.